Proceedings Paper:

Omaruddin, A. and Trodden, P. orcid.org/0000-0002-8787-7432 (2023) LMI-based decentralized load frequency control of a hybrid power system with a virtual synchronous generator and battery storage. In: Ishii, H., Ebihara, Y., Imura, J. and Yamakita, M., (eds.) IFAC-PapersOnLine. 22nd World Congress of the International Federation of Automatic Control (IFAC 2023), 09-14 Jul 2023, Yokohama, Japan. Elsevier , pp. 10910-10916.

https://doi.org/10.1016/j.ifacol.2023.10.775

Available online at www.sciencedirect.com

ScienceDirect

IFAC PapersOnLine 56-2 (2023) 10910–10916

LMI-based Decentralized Load Frequency Control of a Hybrid Power System with a Virtual Synchronous Generator and Battery Storage

Abdulla Omaruddin*, Paul Trodden**

**Nuclear & Power, Atkins, UK (e-mail: Abdulla.Omaruddin@atkinsglobal.com).*

***Department of Automatic Control and Systems Engineering, The University of Sheffield, UK (e-mail: p.trodden@sheffield.ac.uk).*

Abstract: This paper proposes the participation of wind generation in the decentralized control of load frequency of a hybrid power system consisting of, in addition to wind generation, conventional generation and battery storage. The wind generation is modelled as a 'Virtual Synchronous Generator (VSG)' in a separate control area with its own virtual frequency. It has also been proposed to operate the wind generation system in a 'de-loaded' mode, thereby allowing it to take part in frequency regulation services. For the purposes of a decentralized control design, the overall system model is decomposed into three subsystems. Static state-feedback control gains are computed by posing the decentralized control problem as a set of linear matrix inequalities (LMIs) subject to structural and stabilizing constraints.

Keywords: Optimal operation and control of power systems; Control of renewable energy resources; Control system design.

1. INTRODUCTION

Power networks are experiencing a period of rapid transformation due to the increased penetration of renewable technologies such as wind generation and battery storage systems. Such increased penetration, especially of wind, poses significant challenges to the operation and resiliency of the future power system. At a network level, the inertia-less interface provided by the power electronic converters and the intermittency in the renewable supply may result in poor quality supply and even frequency stability issues leading to damage of electrical equipment or, worse, blackouts. Additionally, the increase in the uncontrollable renewable assets is making traditional centralized load frequency control (LFC) schemes challenging to operate: in essence, the intermittency in the renewable generation is 'offloaded' to the grid, thereby stressing it. The described scenario has two main implications. Firstly, the need to develop effective methods that allow renewable generation to take part in frequency regulation. Secondly, motivated by the increasing complexity of the system, the need to devise scalable and practical control approaches, such as decentralized control laws (Bakule, 2008) that account for interconnectivity of the system and the limited information available to operators.

1.1 Wind Generation Modelling and Integration

Various methods of incorporating a wind generation (WG) system for LFC have been proposed in literature. In (Arita et al., 2006), a noise model consisting of band-limited white-noise with filtering was used to model the power output of a wind farm. Though this model provides a rough approximation of the wind power variability, it does not provide an insight into the physics of the wind turbine and hence cannot be utilized effectively in frequency control. A simplified mechanical model of a variable-speed wind turbine was investigated in (Martínez-Lucas et al., 2018). Though the scheme is able to provide short-term inertia in the event of a frequency disturbance, it cannot be incorporated into the LFC design because the proposed PI and PD loops have no direct connection to a dynamical component.

The virtual synchronous generator (VSG) has become widely studied and accepted as a means of connecting inverter-based renewables to the grid while emulating the inertial effect of conventional synchronous generators (Suvarov et al., 2022). The VSG control architecture uses the swing equation to calculate the desired voltage angle and a reactive power control loop to calculate the desired voltage magnitude. Both these quantities are used to produce the pulse-width modulated (PWM) signal to the inverter interfaced with the grid. The reactive power control loop is, however, typically decoupled and disregarded for LFC purposes (Bevrani et al., 2014). This approach is taken in, for example, (da Silva et al., 2020) where, in addition to the swing equation, a virtual mechanical actuator was presented to incorporate primary frequency control (PFC) and secondary frequency control (SFC). This model provides only short-term inertia since the remainder of the control action is cancelled by a low pass filter and an integrator. A similar approach was investigated in (Tessaro and Oliveira, 2019) where PFC and SFC are incorporated into the VSG model. In addition to providing short-term virtual inertia, the VSG adjusts its output power to reduce the steady-state frequency deviation. Neither contribution, however, achieves theoretical guarantees of system stability and control performance, and this is typical of the VSG-supported LFC literature at large (Bevrani et al., 2021).

1.2 Decentralized Load-Frequency Control using LMIs

Decentralized control has been widely studied for applications to LFC; see, for example, the surveys (Ejegi et al., 2014, Ranjan and Shankar, 2022). Among the many techniques

10.1016/j.ifacol.2023.10.775

proposed, optimization-based design methods using Linear Matrix Inequalities (LMIs) have attracted significant attention, owing to their flexibility to handle many control synthesis problems in a tractable and systematic way yet provide stable and effective control. The earliest proposals include (Rerkpreedapong et al., 2003a), where an LMI-tuned PI control law was developed and found, in a three-area LFC scenario, to achieve performance similar to that of a full-order dynamic H_∞ controller. A robust decentralized H_∞ controller, synthesized using LMIs, was computed for one of the control areas in a two-area LFC scenario (Rerkpreedapong et al., 2003b). Its performance was compared with the other area controlled by a conventional PI controller and was found to be superior in terms of transient performance and disturbance rejection. Siljak et al. (2002) considered a multi-machine power system where each machine was represented with a nonlinear differential equation; a nonlinear interconnection term representing the power exchange over a tie-line was assumed to bounded by a quadratic inequality. The robust decentralized control synthesis problem was formulated as a set of LMIs such that the global asymptotic stability is achieved under worst-case uncertainty. Numerous other studies and proposals have followed (Ejegi et al., 2014), achieving a wide range of system theoretic guarantees and performance benchmarks.

1.3 Scope and Contribution

The focus of the current paper is on the decentralized LFC problem for a hybrid power system, wherein conventional generation, WG and battery energy storage (BESS) are desired to be integrated and controlled by independent controllers. Similar to (Tessaro and Oliveira, 2019) and (da Silva et al., 2020), we integrate WG into the LFC problem by modelling it as a VSG in a separate control area, connected via a tie-line cable to the control area containing conventional generation and BESS. We then regard the decentralized control design problem as a structured state-feedback control synthesis problem, and formulate this using LMIs. To achieve this, we adopt and extend a recently developed approach to the structured state-feedback design problem (Ferrante et al. 2020a), which fully relaxed the requirement – typical in decentralized LMI design – to impose particular structure on the Lyapunov matrix in the LMIs in order to achieve desired structure on the feedback gain matrix; the formulation is known to reduce conservatism and succeed in decentralized control law synthesis problems that conventional LMI formulations find infeasible (Ferrante et al., 2020a). An extension (Ferrante et al., 2020b) included an H_∞ performance criterion. The current paper extends the basic approach to consider a quadratic performance criterion in the LMI formulation, thus offering a tractable solution to the structured LQR problem. We achieve this by using a dilation of the Lyapunov inequality (Ebihara et al., 2004) that allows the LQ criterion to be imposed without introducing nonlinear terms.

This paper is organized as follows: Section 2 presents the system model and Section 3 presents the decentralized control synthesis formulation. Section 5 illustrates the application of the proposed method to an example LFC problem and gives simulation results. Section 5 presents the conclusions and highlights areas for future research.

Notation: $\mathbb{R}$ denotes the set of reals, $\mathbb{R}^{m\times n}$ denotes the set of $n \times n$ real matrices, and $\mathbb{S}_+^n$ denotes the set of $n \times n$ symmetric positive definite matrices; negative definiteness of a matrix A is denoted as $A \prec 0$. The set of non-singular $n \times n$ matrices is $\mathcal{R}^k$. The element-wise (Hadamard) product of matrices A and B is $A \circ B$; the Kronecker product of the same is $A \otimes B$. He{A} is shorthand for $A + A^{\mathrm{T}}$.

2. PROBLEM STATEMENT

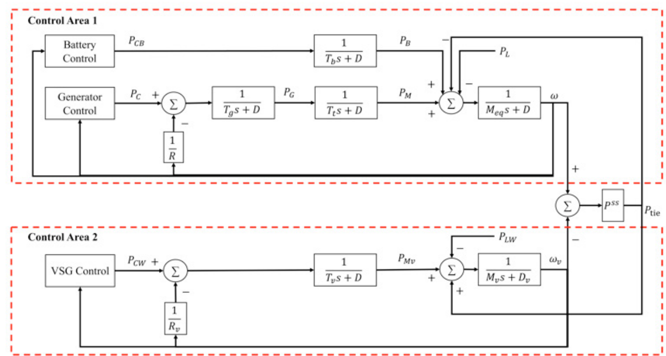

Fig. 1. The hybrid power system incorporating conventional generation, battery storage and wind generation, and the proposed decentralized control architecture.

We consider a hybrid power system, shown in Fig. 1, consisting of two control areas (CAs): the first CA (CA1) consists of conventional generation rated at 2000MVA and BESS rated at 10 MW / 40 MWh. The second CA (CA2) contains the wind generation system, rated at 400MW and operating with a de-loaded factor of 30%, modelled as a VSG connected via a tie-line to the first CA. This abstraction is valid as the system frequency in first control area and the 'virtual' frequency in the second area are separate quantities.

The linearized dynamics of a conventional power system are governed by the swing equation:

$$M_{eq}\frac{d\omega}{dt} = P_M - (P_L + D\omega), \tag{1}$$

where ω is the frequency deviation, M_{eq} is the sum of inertial constants of all generation units, P_M is the mechanical power output of the conventional generator, P_L is the static load change and D is the load damping coefficient (Chow and Sanchez-Gasta, 2020). All variables are expressed as deviations from nominal values.

The mechanical power, P_M, is produced via turbine and governor actions, modelled as

$$T_g\frac{dP_G}{dt} + P_G = P_C - \frac{1}{R}\omega\,, \tag{2}$$

$$T_t\frac{dP_M}{dt} + P_M = P_G. \tag{3}$$

Here the governor output, P_G, is determined by the setpoint, P_C, and the droop (primary control) gain for power sharing, $1/R$. This output is sent to the turbine to produce mechanical power, P_M. The time constants of the governor and turbine are T_g and T_t, respectively.

The BESS is a modelled as a first-order process with an integrator to measure state of charge:

$$T_b \frac{dP_B}{dt} + P_B = P_{CB}, \tag{4}$$

$$\frac{dSOC_B}{dt} = -P_B. \tag{5}$$

Here T_b is the battery time constant, P_B is the battery power output, P_{CB} is the setpoint and SOC_B is the state of charge.

The WG system is modelled with a linearized swing equation and a virtual mechanical actuator with first order dynamics and droop regulation:

$$M_v \frac{d\omega_v}{dt} = P_{Mv} - (P_{LW} + D_v\omega_v), \tag{6}$$

$$T_v \frac{dP_{Mv}}{dt} + P_{Mv} = P_{CW} - \frac{1}{R_v}\omega_v, \tag{7}$$

where ω_v is the virtual frequency deviation, M_v is the virtual inertia, P_{Mv} is the virtual mechanical power output, P_{LW} is the static load on the WG, D_v is the virtual load damping coefficient, and P_{CW} is the setpoint. The interconnection between the WG system and rest of the system is modelled as the tie-line

$$\frac{dP_{\text{tie}}}{dt} = P^{ss}(\omega - \omega_v), \tag{8}$$

where P^{ss} is the line synchronizing coefficient and is related to the physical properties (reactance) of the interconnection between WG and system.

Equations (1)–(8) may be written in compact form as

$$\frac{dx}{dt} = Ax + Bu + Ed, \tag{9}$$

where

$$x := [P_G \quad P_M \quad \omega \quad P_B \quad SOC_B \quad P_{\text{tie}} \quad P_{Mv} \quad \omega_v \quad z_1 \quad z_3]^{\mathrm{T}}$$

$$u := [P_C \quad P_{CB} \quad P_{CW}]^{\mathrm{T}} \text{ and } d := [P_L \quad P_{LW}]^{\mathrm{T}},$$

and, without loss of generality, we have augmented the states with

$$\frac{dz_1}{dt} = -\omega, \frac{dz_3}{dt} = -\omega_v. \tag{10}$$

to facilitate offset-free frequency regulation in the presence of non-zero loads.

The objective is to provide secondary frequency control to maintain the frequency deviation, ω, close to zero, despite the presence of load disturbances, P_L, by manipulating power setpoints, P_C, P_{CB} and P_{CW}. This must be achieved in a decentralized manner where subsystems employ feedback on local states such that the resulting system-wide performance is stable and optimal with respect to a quadratic performance criterion. More precisely, to clarify what is meant by *local* states in this context, consider that (9) is written as

$$\frac{d}{dt}\begin{bmatrix} x_1 \\ x_2 \\ x_3 \end{bmatrix} = \begin{bmatrix} A_{11} & A_{12} & A_{13} \\ A_{21} & A_{22} & A_{23} \\ A_{31} & A_{32} & A_{33} \end{bmatrix}\begin{bmatrix} x_1 \\ x_2 \\ x_3 \end{bmatrix} + \begin{bmatrix} B_1 & 0 & 0 \\ 0 & B_2 & 0 \\ 0 & 0 & B_3 \end{bmatrix}\begin{bmatrix} u_1 \\ u_2 \\ u_3 \end{bmatrix} + \begin{bmatrix} E_1 & 0 \\ 0 & 0 \\ 0 & E_3 \end{bmatrix}\begin{bmatrix} P_L \\ P_{Lw} \end{bmatrix} \tag{11}$$

with local states and inputs

$$x_1 = [P_G \quad P_M \quad \omega \quad P_{\text{tie}} \quad z_1], \qquad u_1 = P_C,$$

$$x_2 = [\omega \quad P_{\text{tie}} \quad P_B \quad SOC_B], \qquad u_2 = P_{CB},$$

$$x_3 = [P_{\text{tie}} \quad P_{Mv} \quad \omega_v \quad z_3], \qquad u_3 = P_{CW}.$$

The decentralized control problem is therefore to design matrices K_1, K_2 and K_3 such that

$$u_i = K_i x_i, i = 1,2,3, \tag{12}$$

stabilizes and provides offset-free control for (9), while minimizing a quadratic performance index

$$\int_0^\infty x^T Q_x x + u^T Q_u u \, dt. \tag{13}$$

3. DECENTRALIZED CONTROL SYNTHESIS

The decomposition depicted in (11) is *overlapping* (Siljak, 1991) in the sense that the three subsystems share some states, namely ω and P_{tie}. The decentralized control law design problem may be cast as one of designing a structured state-feedback control law $u = Kx$: in this case

$$\begin{bmatrix} u_1 \\ u_2 \\ u_3 \end{bmatrix} = \underbrace{\begin{bmatrix} K_1 & 0 & 0 \\ 0 & K_2 & 0 \\ 0 & 0 & K_3 \end{bmatrix}}_{K_D}\begin{bmatrix} x_1 \\ x_2 \\ x_3 \end{bmatrix} \Rightarrow u = \underbrace{K_D M}_{K} x \tag{14}$$

where M determines the overlapping decomposition of states. The gain matrix $K = K_D M$ satisfies a *structural constraint* (Ferrante et al. 2020a) $K \in \mathcal{S}$, where

$$\mathcal{S} = \{K \in \mathbb{R}^{mxn}: K \circ \mathcal{S}(B^{\mathrm{T}}) = 0\}, \tag{15a}$$

$$\mathcal{S}(B^{\mathrm{T}})_{ij} := \begin{cases} 0 \text{ if } B_{ij} \neq 0, \\ 1 \text{ otherwise} \end{cases} \tag{15b}$$

The structured control problem is to then find a $K \in \mathcal{S}$ and $P \in \mathbb{S}_+^n$ satisfying the bilinear matrix inequality (BMI)

$$(A + BK)P + P(A + BK)^{\mathrm{T}} \prec 0. \tag{16}$$

It is well known (Boyd et al., 1994) that (16) converts to a linear matrix inequality (LMI) via the change of variable $K = YP^{-1}$:

$$(AP + BY) + (AP + BY)^{\mathrm{T}} \prec 0. \tag{17}$$

Finding a $K \in \mathcal{S}$ that satisfies (17) is conventionally achieved by imposing structural constraints on P, which is conservative and may fail to find a feasible solution even when decentralized stabilizability of the system is possible. This limitation was overcome by Ferrante at al. (2020a), who proposed a novel dilation of (17) in order that no structure need be imposed on the matrix P other than positive definiteness. The proposal is characterized by the following result.

Theorem 1. (Ferrante et al. 2020a) Let $\{\mathcal{S}_1, \dots, \mathcal{S}_k\}$ be a basis for $\mathcal{S}$, let

$$L := [\mathcal{S}_1 \quad \mathcal{S}_2 \quad \cdots \quad \mathcal{S}_k] \tag{18}$$

and define the structured set

$$\Upsilon := \{X \in \mathcal{R}^n : \exists \Lambda \in \mathcal{R}^k \; s.t. \, L(I_k \otimes Q) = L(\Lambda \otimes I_n)\}.$$

If there exists a $P \in \mathbb{S}_+^n$, an $R \in \mathcal{S}$ and an $X \in \Upsilon$ such that

$$\begin{bmatrix} 0 & P \\ P & 0 \end{bmatrix} + \mathrm{He}\left\{\begin{bmatrix} AX + BR & AX + BR \\ -X & -X \end{bmatrix}\right\} \prec 0 \tag{19}$$

then $K = RX^{-1} \in \mathcal{S}$ solves (16).

Theorem 1 solves the structured state-feedback control problem with respect to stability but omits any performance criterion; an extension of the method (Ferrante et al. 2020b) minimizes the H_∞ performance criterion. In this paper, in a similar vein, we extend the result of Ferrante et al. (2020a) to minimize or bound the H_2 norm of the closed-loop system, resulting in a solution to the structured H_2 state-feedback synthesis problem. This naturally includes the case of minimizing an LQ-type cost function, thus also offering a solution to the structured LQR problem. Unfortunately, adapting (19) directly to include the H_2/LQR performance criterion is not straightforward, resulting in nonlinear terms. We therefore achieve the extension by using an alternative dilation of the Lyapunov inequality in the H_2 formulation, due to Ebihara and Hagiwara (2004), and combining this with the structural constraints in Theorem 1.

Consider a system

$$\frac{dx}{dt} = Ax + Bu + Ed \tag{20a}$$

$$y = Cx + Du \tag{20b}$$

whose transfer function under state feedback $u = Kx$ is

$$H(s) = (C + DK)[sI - (A + BK)]^{-1}E \tag{21}$$

with H_2 norm $\|H(s)\|_2$. The following result solves the structured state feedback control synthesis problem while bounding the H_2 norm.

Theorem 2. If for some $b > 0$, there exists a $P \in \mathbb{S}_+^n$, an $R \in \mathcal{S}$, an $X \in \Upsilon$, and a $Z \in \mathbb{S}_+^n$ such that

$$\begin{bmatrix} 0 & P & 0 \\ P & 0 & 0 \\ 0 & 0 & -I \end{bmatrix} + \mathrm{He}\left\{\begin{bmatrix} AX + BR & b(AX + BR) & 0 \\ -X & -bX & 0 \\ CX + DR & b(CX + DR) & 0 \end{bmatrix}\right\} \prec 0 \tag{22}$$

$$\begin{bmatrix} Z & E^{\mathrm{T}} \\ E & Y \end{bmatrix} \succ 0, \tag{23}$$

$$\mathrm{trace}(Z) < \gamma, \tag{24}$$

then $K = RX^{-1} \in \mathcal{S}$ results in $A + BK$ Hurwitz with $\|H(s)\|_2 < \gamma$.

Proof. Re-writing the left-hand side of (22) as

$$\underbrace{\begin{bmatrix} 0 & P & 0 \\ P & 0 & 0 \\ 0 & 0 & -I \end{bmatrix}}_{\mathcal{L}_1} + \mathrm{He}\left\{\underbrace{\begin{bmatrix} A + BK \\ -I \\ C + DK \end{bmatrix} X [I \quad bI \quad 0]}_{\mathcal{L}_2}\right\} \prec 0$$

and defining the congruence transformation

$$T := \begin{bmatrix} -I & -(A + BK) & 0 \\ 0 & C + DK & I \end{bmatrix}, \tag{25}$$

it follows that

$$T(\mathcal{L}_1 + \mathcal{L}_2 + \mathcal{L}_2^{\mathrm{T}})T^{\mathrm{T}} = T\mathcal{L}_1 T^{\mathrm{T}} \tag{26}$$

since $T\mathcal{L}_2 = 0$ and $\mathcal{L}_2^{\mathrm{T}} T^{\mathrm{T}} = 0$. Therefore, condition (22) is equivalent to

$$\begin{bmatrix} (A + BK)P + P(A + BK)^{\mathrm{T}} & P(C + DK)^T \\ (C + DK)P & -I \end{bmatrix} \prec 0.$$

This, when taken with (23) and (24), gives the standard LMIs for state feedback synthesis with bounded H_2 norm. The block structure of $K = RX^{-1}$ is assured by the constraints $K \in \mathcal{S}$ and $X \in \Upsilon$ (Ferrante et al., 2020a). ■

Theorem 2 is easily adapted to cover the minimization of the quadratic index (13), by setting $E = I$, $C = \begin{bmatrix} Q_x{}^{1/2} & 0 \end{bmatrix}^{\mathrm{T}}$ and $D = \begin{bmatrix} 0 & Q_u{}^{1/2} \end{bmatrix}^{\mathrm{T}}$.

Corollary 1. The LMI formulation that solves the structured LQ problem is

$$\min_{P,X,R} -\mathrm{trace}(P) \tag{27}$$

subject to $P \in \mathbb{S}_{+}^{n}$, $R \in \mathcal{S}$, $X \in \Upsilon$, and

$$\begin{bmatrix} 0 & P & 0 & 0 \\ P & 0 & 0 & 0 \\ 0 & 0 & -I & 0 \\ 0 & 0 & 0 & -I \end{bmatrix} + \text{He}\left\{ \begin{bmatrix} AX+BR & b(AX+BR) & 0 \\ -X & -bX & 0 \\ {Q_x}^{1/2}X & b{Q_x}^{1/2}X & 0 \\ {Q_u}^{1/2}R & b{Q_u}^{1/2}R & 0 \end{bmatrix} \right\} \prec 0.$$

4. APPLICATION TO HYBRID LFC PROBLEM

The decentralized control synthesis method is demonstrated by application to the hybrid LFC problem depicted in Section 2. We consider a power system with the parameters, expressed relative to the based machine rating of 2000MVA

$$M_{eq} = 11.94\text{ s}, M_v = 2.24\text{ s}, D = 0.3549, D_v = 0.36$$

$$T_b = 0.3\text{ s}, T_g = 0.1\text{ s}, T_t = 0.35\text{ s}, T_v = 0.6\text{ s}$$

$$R = 0.037\text{ p.u.}, R_v = 15\text{ p.u.}, P_{\text{tie}} = 3\text{ p.u.}$$

For the decentralized control design, the gain matrix has the desired form

$$K = \begin{bmatrix} K_{11} & K_{12} & K_{13} & 0 & 0 & K_{14} & 0 & 0 & K_{15} & 0 \\ 0 & 0 & K_{21} & K_{22} & K_{23} & K_{24} & 0 & 0 & 0 & 0 \\ 0 & 0 & 0 & 0 & 0 & K_{31} & K_{32} & K_{33} & 0 & K_{34} \end{bmatrix}$$

where each $K_{ij} \in \mathbb{R}$, leading to a 13-element basis for set $\mathcal{S}$. Following the definition of the set Υ, a matrix $X \in \Upsilon$ takes the form

$$\begin{bmatrix} x_{1,1} & x_{1,2} & x_{1,3} & 0 & 0 & x_{1,6} & 0 & 0 & x_{1,9} & 0 \\ x_{2,1} & x_{2,2} & x_{2,3} & 0 & 0 & x_{2,6} & 0 & 0 & x_{2,9} & 0 \\ 0 & 0 & x_{3,3} & 0 & 0 & x_{3,6} & 0 & 0 & 0 & 0 \\ 0 & 0 & x_{4,3} & x_{4,4} & x_{4,5} & x_{4,6} & 0 & 0 & 0 & 0 \\ 0 & 0 & x_{5,3} & x_{5,4} & x_{5,5} & x_{5,6} & 0 & 0 & 0 & 0 \\ 0 & 0 & 0 & 0 & 0 & x_{6,6} & 0 & 0 & 0 & 0 \\ 0 & 0 & 0 & 0 & 0 & x_{7,6} & x_{7,7} & x_{7,8} & 0 & x_{7,10} \\ 0 & 0 & 0 & 0 & 0 & x_{8,6} & x_{8,7} & x_{8,8} & 0 & x_{8,10} \\ x_{9,1} & x_{9,2} & x_{9,3} & 0 & 0 & x_{9,6} & 0 & 0 & x_{9,9} & 0 \\ 0 & 0 & 0 & 0 & 0 & x_{10,6} & x_{10,7} & x_{10,8} & 0 & x_{10,10} \end{bmatrix}$$

where each $x_{ij} \in \mathbb{R}$. The matrix R has the same structure as K. Thus, X has a structure that results in RX^{-1} having the desired structure for K, but no structure is imposed on P.

We design the structured K to minimize the quadratic performance criterion (11) with

$$Q_x = \text{diag}(1,0.7,100,0.001,0.001,1,10,100,85,85),$$

$$Q_u = \text{diag}(0.0001,0.0001,1),$$

thus penalizing most heavily the real and virtual frequency deviations and their integrated values. For comparison, we also design a centralized state feedback control law using LQR (using the same cost function matrices – omitting the final element in Q_x for reference tracking in real frequency deviation only) applied to the whole system, and a set of decentralized LQR control laws by considering the decoupled dynamics of each subsystem, i.e.,

$$\frac{dx_i}{dt} = A_{ii}x_i + B_i u_i, \tag{28}$$

such that interactions $\sum_{j\neq i} A_{ij}x_j$ are ignored. Note that for decentralized LQR, only reference tracking of virtual frequency deviation was included for satisfactory system response.

Fig. 2 shows the frequency response of the system following a load disturbance $P_L = 0.01\text{ p.u.}$ (20 MW) in CA1 at $t = 10$ s. Figs. 3 and 4 show the corresponding generation asset outputs and BESS power output. The centralized LQR achieves the optimal response for this set of weighting matrices. The two decentralized schemes produce a longer settling time albeit with a smaller frequency nadir. All three control schemes engage the WG asset, but to differing amounts; the proposed LMI-based control law makes maximal use of the WG in steady state. The BESS supports the frequency only during the initial transient; however, the decentralized LQR scheme discharges the BESS most ($SOC_B = 0$ corresponds to a nominal initial charge) while the decentralized LMI scheme resembles the response from the centralized LQR scheme, despite the absence of communication between the subsystem controllers.

Fig. 5 shows the frequency response of the system following a load disturbance $P_L = 0.01\text{ p.u.}$ (20 MW) in CA2 at $t = 10$ s. Figs. 6 and 7 show the corresponding generation asset outputs and BESS power output. The proposed LMI-based control laws achieve the smallest frequency nadir but a settling time longer than the centralized control law, as was also observed for a disturbance in CA1. Both decentralized LQR and the proposed LMI-based control laws maximize the use of the VSG. However, both under-utilize the BESS. This is expected as there is no information exchange between the controllers (i.e. the controllers are acting on local information). In the case of the proposed LMI-based control laws, both the conventional generation and the BESS reduce their power output (charge in the case of the BESS) to accommodate the sharp increase in the power output of the VSG, as shown in Fig. 6 and 7.

The closed loop cost was calculated for each of the above-mentioned schemes using the same cost function matrices – omitting the final element in Q_x in the case of centralized and decentralized LQR. The results are in line with our intuition. That is, the centralized implementation has the lowest cost followed by the decentralized control laws.

Table 1. Closed Loop Costs

Control Scheme	Disturbance in CA1	Disturbance in CA2
Centralized LQR	0.2486	0.3153
Decentralized LQR	0.6334	12.2517
Decentralized LMI	0.6724	2.7204

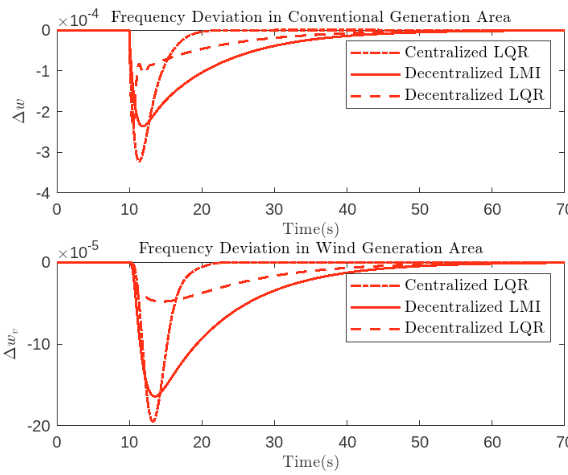

Fig. 2. Frequency response to a load disturbance of $\Delta P_L = 0.01$ p. u. (20 MW) in CA1 at $t = 10\ s$.

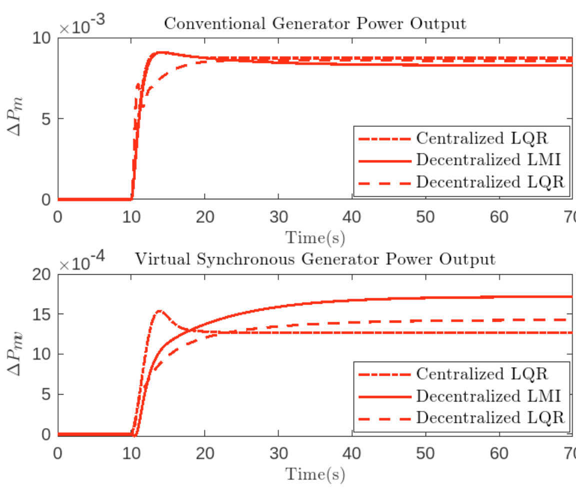

Fig. 3. Power outputs of generators during a load disturbance of $\Delta P_L = 0.01$ p. u. (20 MW) in CA1 at $t = 10\ s$.

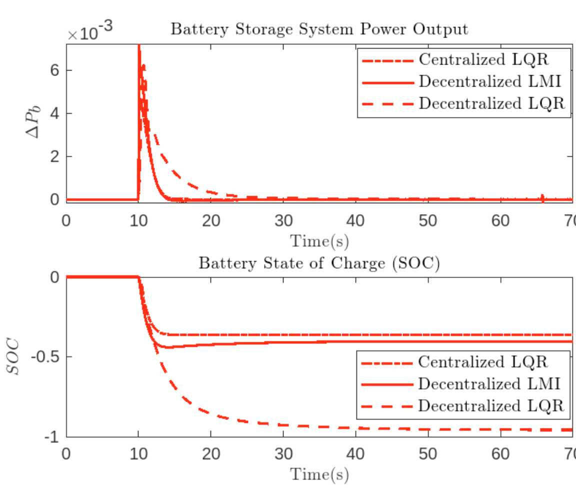

Fig. 4. BESS power output and state of charge during a load disturbance $\Delta P_L = 0.01$ p. u. (20 MW) in CA1 at $t = 10\ s$.

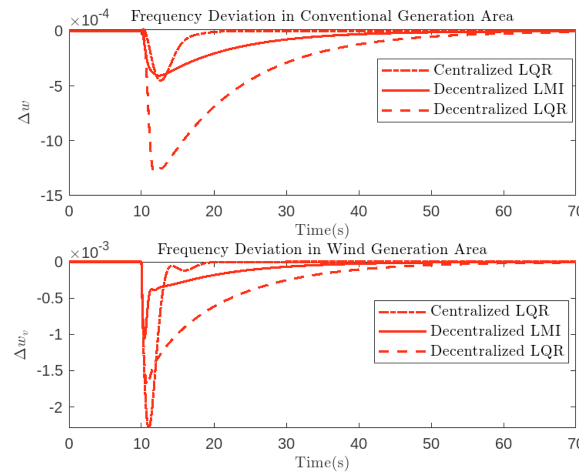

Fig. 5. Frequency response to a load disturbance of $\Delta P_L = 0.01$ p. u. (20 MW) in CA2 at $t = 10\ s$.

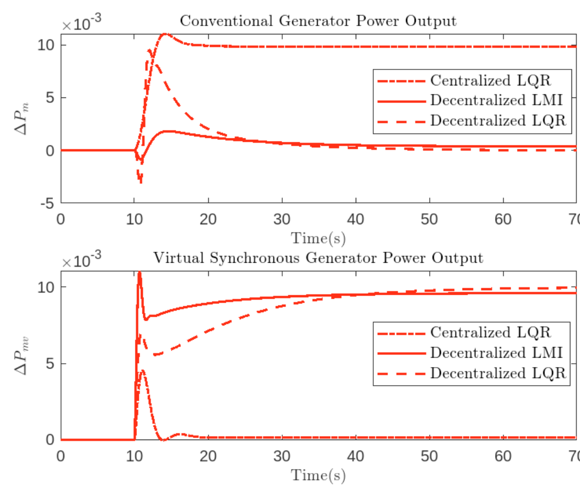

Fig. 6. Power outputs of generators during a load disturbance of $\Delta P_L = 0.01$ p. u. (20 MW) in CA2 at $t = 10\ s$.

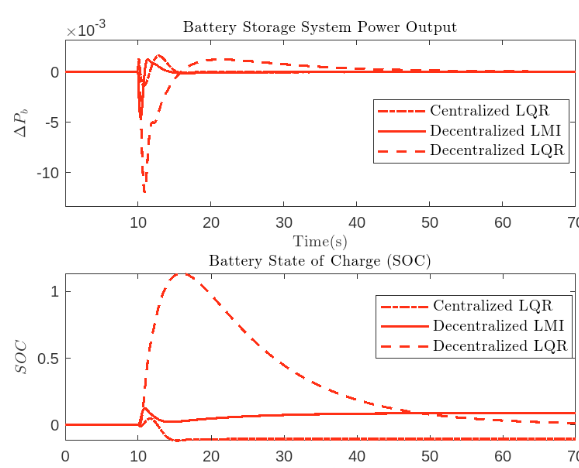

Fig. 7. BESS power output and state of charge during a load disturbance $\Delta P_L = 0.01$ p. u. (20 MW) in CA2 at $t = 10\ s$.

5. CONCLUSION

This paper has considered the secondary control design problem for a power system incorporating VSG-connected WG and BESS. We proposed an extension of a structured control synthesis method (Ferrante et al., 2020a) to formulate the optimal H2/LQR decentralized control design problem via LMIs. This achieves a systematic design of stable optimal decentralized control laws. We applied the results to design stable-decentralized control gains for a hybrid power system example. The performance of the LMI-based scheme was seen to out-perform that of an ad-hoc decentralized LQR scheme, with significant benefit of stability by design.

REFERENCES

Arita, M., Yokoyama, A. and Tada, Y. (2006). Evaluation of Battery System for Frequency Control in Interconnected Power System with a Large Penetration of Wind Power Generation. *2006 International Conference on Power System Technology*, pp. 1–7.

Bakule, L. (2008). Decentralized control: An overview. *Annual Reviews in Control*, 32(1), pp.87–98.

Bevrani, H., Ise, T., Miura, Y. (2014). Virtual synchronous generators: A survey and new perspectives. International Journal of Electrical Power & Energy Systems, 54, pp. 244–254.

Bevrani, H., Golpîra, H., Messina, A.R., Hatziargyriou, N., Milano, F. and Ise, T. (2021). Power system frequency control: An updated review of current solutions and new challenges. *Electric Power Systems Research*, 194, 107114.

Boyd, S., El Ghaoui, E. Feron, and Balakrishnan, V. (1994). *Linear Matrix Inequalities in Systems and Control Theory.* Ser. Studies in Applied Mathematics. Philadelphia, PA: SIAM, vol. 15.

Chow, J. and Sanchez-Gasca, J. (2020). Power System Modeling, Computation, and Control. *Newark: John Wiley & Sons, Incorporated*, pp.327–365.

da Silva, G., de Oliveira, E., de Oliveira, L., de Paula, A., Ferreira, J. and Honório, L. (2021). Load frequency control and tie-line damping via virtual synchronous generator. *International Journal of Electrical Power & Energy Systems*, 132, p.107108.

Ebihara, Y. and Hagiwara, T. (2004). New dilated LMI characterizations for continuous-time multi-objective controller synthesis. *Automatica*, vol. 40, no. 11, pp. 2003–2009.

Ejegi, E. E., Rossiter, J. A. and Trodden, P. (2014). A survey of techniques and opportunities in power system automatic generation control. *2014 UKACC International Conference on Control (CONTROL)*, pp. 537–542.

Ferrante, F., Dabbene, F. and Ravazzi, C. (2020a). On the Design of Structured Stabilizers for LTI Systems. *IEEE Control Systems Letters*, 4(2), pp.289–294.

Ferrante, F., Dabbene, F. and Ravazzi, C. (2020b). An LMI Approach for Structured $\mathcal{H}_\infty$ State Feedback Control. *IFAC PapersOnLine*, 53-2, 4058–4063.

Martínez-Lucas, G., Sarasúa, J. and Sánchez-Fernández, J. (2018). Eigen analysis of wind–hydro joint frequency regulation in an isolated power system. *International Journal of Electrical Power & Energy Systems*, 103, pp. 511–524.

Ranjan, M., Shankar, R. (2022). A literature survey on load frequency control considering renewable energy integration in power system: Recent trends and future prospects. *Journal of Energy Storage*, 45, 103717.

Rerkpreedapong, D., Hasanovic, A. and Feliachi, A. (2003a). Robust load frequency control using genetic algorithms and linear matrix inequalities. *IEEE Transactions on Power Systems*, 18(2), pp. 855–861.

Rerkpreedapong, D. and Feliachi, A. (2003b). Decentralized $\mathcal{H}_\infty$ load frequency control using LMI control toolbox. *Proceedings of the 2003 International Symposium on Circuits and Systems, 2003. ISCAS'03*. (Vol. 3, pp. III-III). IEEE.

Siljak, D. (1991). *Decentralized control of complex systems*. Boston, Mass.: Academic Press.

Siljak, D., Stipanovic, D. and Zecevic, A. (2002). Robust decentralized turbine/governor control using linear matrix inequalities. *IEEE Transactions on Power Systems*, 17(3), pp.715–722.

Suvorov, A., Askarov, A., Kievets, A. and Rudnik, V. (2022). A comprehensive assessment of the state-of-the-art virtual synchronous generator models. *Electric Power Systems Research*, 209, 108054,

Tessaro, H. and Oliveira, R. (2019). Impact assessment of virtual synchronous generator on the electromechanical dynamics of type 4 wind turbine generators. *IET Generation, Transmission & Distribution*, 13(23), pp.5294–5304.